ELSEVIER

An analytical model of stand dynamics as a function of tree growth, mortality and recruitment: The shade tolerance-stand structure hypothesis revisited

Miguel A. Zavala[a,*], Óscar Angulo[b], Rafael Bravo de la Parra[c], Juan C. López-Marcos[b]

[a]Dpto. de Ecología, Universidad de Alcalá, E-28871, Alcalá de Henares (Madrid), Spain
[b]Dpto. de Matemática Aplicada, Universidad de Valladolid, Spain
[c]Dpto. de Matemáticas, Universidad de Alcalá, E-28871, Alcalá de Henares (Madrid), Spain

Abstract

Light competition and interspecific differences in shade tolerance are considered key determinants of forest stand structure and dynamics. Specifically two main stand diameter distribution types as a function of shade tolerance have been proposed based on empirical observations. All-aged stands of shade tolerant species tend to have steeply descending, monotonic diameter distributions (inverse J-shaped curves). Shade intolerant species in contrast typically exhibit normal (unimodal) tree diameter distributions due to high mortality rates of smaller suppressed trees. In this study we explore the generality of this hypothesis which implies a causal relationship between light competition or shade tolerance and stand structure. For this purpose we formulate a partial differential equation system of stand dynamics as a function of individual tree growth, recruitment and mortality which allows us to explore possible individual-based mechanisms—e.g. light competition—underlying observed patterns of stand structure—e.g. unimodal or inverse J-shaped equilibrium diameter curves. We find that contrary to expectations interspecific differences in growth patterns can result alone in any of the two diameter distributions types observed in the field. In particular, slow growing species can present unimodal equilibrium curves even in the absence of light competition. Moreover, light competition and shade intolerance evaluated both at the tree growth and mortality stages did not have a significant impact on stand structure that tended to converge systematically towards an inverse J-shaped curves for most tree growth scenarios. Realistic transient stand dynamics for even aged stands of shade intolerant species (unimodal curves) were only obtained when recruitment was completely suppressed, providing further evidence on the critical role played by juvenile stages of tree development (e.g. the sapling stage) on final forest structure and composition. The results also point out the relevance of partial differential equations systems as a tool for exploring the individual-level mechanisms underpinning forest structure, particularly in relation to more complex forest simulation models that are more difficult to analyze and to interpret from a biological point of view.
© 2006 Elsevier Ltd. All rights reserved.

Keywords: Shade tolerance; Recruitment; Growth; Mortality; Light competition

1. Introduction

Understanding the collective behaviour of plant communities and populations in terms of individual performance is a central goal of theoretical ecology (Harper, 1977; Crawley, 1986). In the case of forest ecosystems examination of the mechanisms governing stand structure and dynamics has also been central for the development of silviculture and forest management (Smith, 1962; Oliver and Larson, 1990). A stand is defined as a spatially homogeneous unit of arbitrary size within a forest (Oliver and Larson, 1990). Its structure is characterized by the frequency distribution of tree diameters which results from several factors such as disturbance history, species physiology, competition as well as site ecological conditions (Bailey and Dell, 1973; Kohyama, 1991a, b). One of the most widely accepted mechanism for divergence in stand structure is based on species differential responses to light suppression or shade tolerance (e.g. Lorimer and Krug, 1983). Specifically three main diameter distribution types as a function of shade tolerance have been proposed: all-aged

*Corresponding author. Tel.: +34 615 689 489.
E-mail address: ma.zavala@uah.es (M.A. Zavala).

stands of shade tolerant species with only light past disturbance tend to have steeply descending, monotonic diameter distributions that can be approximated by negative exponential and negative power functions (Assman, 1970; Liocurt, 1898; Lorimer, 1980; Abrams and Downs, 1990). Shade intolerant species typically exhibit normal tree diameter distributions due to high mortality rates of smaller suppressed trees (Glitzenstein et al., 1986; Knox et al., 1989). Third, a combination of the other two types of curves can be found depending on stand history and species shade tolerance, including curves with a steeply descending monotone in the understory diameter classes and a broad peak in the overstory classes, to multi-modal tree diameter distributions (Parker, 1984; Lorimer and Krug, 1983). Also according to silvicultural theory the dynamics of stand structure in even aged stands follows a characteristic sequence from initial colonization pattern (inverse J-shaped curve or sharp unimodal distribution centred in smaller size classes) to a flattening unimodal (or bi-modal) distribution with positive skewness and a gradually increasing mean (Lanier, 1986).

The generality of these patterns and the underlying mechanisms, however, are a matter of debate (Lorimer and Krug, 1983; Lischke, 2001; Binkley et al., 2002) and a general mechanistic explanation of emergence of stand structure and dynamics patterns remains elusive. Over the last decades significant progress has been made on the formulation of analytical models for size-structured populations (Hara, 1984a, b; Kohyama, 1991a, b; Calsina and Saldaña, 1997), numerical techniques for their analyses (Metz and Diekmann, 1986; De Roos, 1997, Angulo and López-Marcos, 1999, 2000, 2002, 2004), and characterization of whole plant responses to shade (Canham, 1989; Kobe et al., 1995). These advances facilitate the development of realistic analytical models of stand structure and dynamics as a function of individual-based process.

In this study, we use a partial differential equation system in which growth, recruitment and mortality rates are based on measurable parameters in the field and we investigate the mechanisms that govern stand structure and dynamics in moderately disturbed stands. Individual-based forest simulators (Shugart, 1984; Tilman, 1988; Pacala et al., 1996) are usually more realistic from a biological point of view than analytical models, but complexity may make the analysis difficult. We therefore follow a minimalist approach (i.e. sensu Casagrandi and Rinaldi, 1999) to identify the simplest mechanisms that account for observed patterns. We use recent developments in numerical analysis to explore the connection between models of increasing complexity and predicted patterns. We first investigate whether differences in species growth patterns can alone explain changes in stand structure even in the absence of tree to tree competition. Secondly, we examine whether shifts from unimodal to inverse J-shaped distribution curves and vice versa can be explained by individual responses to asymmetric (light) competition. We evaluate this separately when competition is expressed at the growth

and the mortality stages. Finally, we investigate under which conditions (e.g. parameter values for recruitment, growth and mortality) realistic patterns of stand dynamics for even aged stands of shade intolerant species can be obtained. This is to our knowledge the first study in which the relationship between stand structure and shade tolerance is theoretically evaluated with an analytical model of stand dynamics.

2. Model description

Zavala and Bravo de la Parra (2005) propose a general analytical framework to describe stand dynamics by means of a general multi-species model of a size-structured tree population which takes into account the effects of competition for light and water. Here we treat the particular case of a mono-species model of size-structured tree population and we focus on one-sided competition (i.e. light), a primary ecological factor underlying forest succession in temperate and tropical forests (Shugart, 1984; Valladares, 2003).

Both independent variables size x and time t are considered continuous. The size variable x represents, following Kohyama (1991b, 1992), the d.b.h. (diameter at breast height). Let $u(x, t)$ be the population density with respect to d.b.h. of trees in the stand per m^2, what means that

$$\int_{x_1}^{x_2} u(\sigma, t)\, d\sigma$$

represents the number of trees in the stand patch per m^2 with d.b.h. $x \in [x_1, x_2]$ at time t.

The cumulative basal area of trees greater in size than x expresses the shading effect under one-sided competition and it is defined by

$$B(x, t) = \int_x^{x_M} \frac{\pi}{4} \sigma^2 u(\sigma, t)\, d\sigma \tag{1}$$

and x_M is the maximum d.b.h. reached by a given tree species. If we denote x_0 the minimum d.b.h. for a tree to be considered a recruit, then $B(x_0, t)$ represents the total basal area of the trees in the stand per m^2.

Changes in size distribution depend on the rates of size growth, mortality and recruitment. We are now presenting all these rates in full generality.

Growth rate:

$$G(x, B(x, t)),$$

where $G(x, z)$ is, in general, a unimodal function tending to 0 when x tends to x_M for constant z. For constant x, $G(x, z)$ is a monotonous decreasing function of z

Mortality rate:

In general

$$M(x, B(x, t)),$$

where $M(x, z)$ is a function which is increasing for constant x.

Recruitment rate:

A general recruitment rate can be expressed in the following form:

$$R(t) = B(x_0, t)r(B(x_0, t)), \tag{2}$$

which is proportional to total basal area and where $r(z)$ is a decreasing function reflecting density-dependent effects. The outcome of these two opposed forces—increasing seed production and decreasing seedling survival with increasing basal area—on recruitment is rather system-specific and largely depends on system-specific mechanisms (e.g. seed predation in tropical humid forests, Hubbell, 1980; or water stress in Mediterranean forests, Lookingbill and Zavala, 2000). Moreover, net recruitment rate depends in a spatial context on dispersal rates from nearby stands, so it changes with regional species abundance and dispersal mode (Pacala et al., 1996). Thus, for the purpose of this study we assume that recruitment is a free constant parameter. We also consider the specific case of null recruitment as most documented patterns in stand dynamics refer to relatively shorter time periods in relation to time periods required for models to reach a mathematical equilibrium (e.g. one rotation cycle in managed forests). Recruitment limitation is a rather common phenomenon both in managed and natural plant communities (e.g., Espelta et al., 1995; Hurtt and Pacala, 1995; Turnbull et al., 2000). Thus, in the sequel recruitment rate will be considered either a positive constant for cases with continuous recruitment, or zero.

The general continuum model based upon the classical model for a state-structured population (Metz and Diekmann, 1986; Cushing, 1998) reads as follows:

Balance law

$$u_t(x, t) + (G(x, B(x, t))u(x, t))_x$$
$$= -M(x, B(x, t))u(x, t) \quad (x_0 < x < x_M, t > 0). \tag{3}$$

Recruitment law

$$G(x_0, B(x_0, t))u(x_0, t) = B(x_0, t)r(B(x_0, t)) \quad (t > 0). \tag{4}$$

Initial d.b.h. distribution

$$u(x, 0) = u_0(x) \quad (x_0 \leqslant x \leqslant x_M). \tag{5}$$

These kind of models has been used by many authors in plant ecology (Nagano, 1978; Hara, 1984a, b, 1985, 1992; Takada and Iwasa, 1986; Kohyama, 1991a, b, 1992; Hara and Yokozawa, 1994; Kraev, 2001; Dercole et al., 2005) as well as in various other fields of biology (Von Foerster, 1959), demography (Keyfitz, 1968) and epidemiology (Kermack and McKendrick, 1933) to cite just the pioneers. Likewise, the Sharpe–Lotka–McKendrick equation is a particular version of the more general Fokker–Plank equation (also known as diffusion or Kolmogorov forward equation) to incorporate the spatial and stochastic fluctuations of the size density distribution, see Hara (1984a, b, 1985, 1992). The original Sharpe–Lotka–McKendrick equation is linear. Nonlinear age- and size-structured population models arise when any of the population rates (growth, birth, death) depend on the population density or

on a functional of it as in Eqs. (3) and (4). The first study of a nonlinear age-structured model is developed by Gurtin and MacCamy (1974); a comprehensive treatment of their approach, based on Volterra integral equations, is given by Iannelli (1994). Other fruitful approach for the study of linear and nonlinear structured models is based on the theory of semigroups of linear and nonlinear operators in Banach spaces, see Webb (1985) as the fundamental reference for age-structured populations; the case of size-structured population is treated in Metz and Diekmann (1986) and Cushing (1998), and the combination of age- and size-structured models is studied in Shinko and Streifer (1967) and Tucker and Zimmerman (1988).

Often models such as those discussed above cannot be solved analytically and require numerical integration to obtain an approximation of the solution. In addition, the precise form of many of the life history functions of a population are often hard to determine, and the use of a numerical scheme may assist their approximation by comparisons with field data. A number of numerical schemes exist, primarily for age rather than size structured models. Two main numerical procedures have been considered. The first one is based on standard difference schemes used to approximate partial differential equations (upwind, box, Lax-Wendroff, Warming-Beam, method of lines, etc.) with adjustments to cope with non-local terms. The second one, and most popular, approach is based upon integration along characteristic curves and seeks to solve the resulting coupled system of ordinary differential equations. Two categories of this kind of methods have been considered: Runge–Kutta/multi-step methods and the method for discretization of a representation of the solution along characteristics, see Abia et al. (2004, 2005) for a comparison of different numerical methods with regards to accuracy, efficiency, generality and mathematical methodology.

Modern numerical methods have been successfully applied to structured models to replicate available field and/or laboratory data, for a variety of different systems. Most of them has been considered in the case of age-structured populations. A size-structured population model for *Gambussia affinis* with seasonal dependence was introduced and numerically studied by Sulsky (1994). With the use of a more efficient numerical method, Angulo et al. (2005) showed new properties of the model for long times, such as the tendency to periodicity. Finally, in Bees et al. (2006), a nonlinear structured population model for the slug *Deroceras reticulatum* has been numerically explore with conclusions about the diagnostic to distinguish between predated and non-predated environments. All these works indicate that structured population models and numerical simulations are valid tools for investigating systems such as the one under consideration here.

In Appendix A it is presented the numerical method employed in this paper. It is a new scheme that for the first time discretizes this type of hierarchical size-structured model. It employs a representation of the solution along

the characteristics and also uses a selection of grid nodes in order to improve its efficiency.

3. Model analysis, simulations and results

3.1. Tree growth without light competition and stand structure

We assume that the recruitment rate, R, and the mortality rate, μ, are constant. On the other hand, all trees in the stand increase their d.b.h. x over time in the same way, as governed by a growth function $g(x)$ satisfying the following hypotheses: $g : [x_0, x_M] \rightarrow [0, \infty)$ is continuous, positive on (x_0, x_M), $g(x_0) > 0$, $g(x_M) = 0$ and $\int_{x_0}^{x_M} d\sigma / g(\sigma) = \infty$.

Under these assumptions system (3)–(5) reads as follows:

$$u_t(x, t) + (g(x)u(x, t))_x = -\mu u(x, t)$$
$$(x_0 < x < x_M, \ t > 0), \tag{6}$$

$$g(x_0)u(x_0, t) = R \quad (t > 0), \tag{7}$$

$$u(x, 0) = u_0(x) \quad (x_0 \leqslant x \leqslant x_M). \tag{8}$$

System (6)–(8) can be solved analytically by the characteristics method which is described at the beginning of Appendix A. The solution is expressed in terms of the function defining the characteristic line of Eq. (6) through the point $(x_0, 0)$ which is

$$\int_{x_0}^{x} \frac{d\sigma}{g(\sigma)} = t \tag{9}$$

denoted $t = \varphi(x)$. The function $\varphi(x)$ represents the time required for a tree to increase d.b.h. from x_0 to x. The hypotheses assumed on $g(x)$ imply that trees grow from any d.b.h. $x \geqslant x_0$ approaching the maximum d.b.h. x_M but never attaining it, as time goes to ∞. They also imply that the inverse of $\varphi(x)$ exists, $\varphi^{-1}(t)$ defined on $[0, \infty)$.

The solution of system (6)–(8) is

$$u(x, t) = \begin{cases} u_0(\varphi^{-1}(\varphi(x) - t))e^{-\mu t} \dfrac{g(\varphi^{-1}(\varphi(x) - t))}{g(x)} & \text{if } \varphi(x) > t, \\ R \dfrac{\exp(-\mu \varphi(x))}{g(x)} & \text{if } \varphi(x) < t, \end{cases} \tag{10}$$

which tends uniformly on any interval $[x_0, x]$, with $x < x_M$, to the steady state solution

$$u^*(x) = R \frac{\exp(-\mu \varphi(x))}{g(x)} \tag{11}$$

representing the long term d.b.h. distribution of trees in the stand. The different types of equilibrium curves observed in the field could be explained through this model just by the type of growing associated with the corresponding species and environment, that is, without any mechanism related to competition for light. This is the case because as we see $u^*(x)$ depends on $g(x)$, the individual growth rate, and for a given d.b.h. distribution of trees we could find a $g(x)$ yielding it as steady state solution. A straightforward computation gives for a d.b.h. distribution $\phi(x)$ the

following growth rate:

$$g(x) = \frac{1}{\phi(x)} \left(R - \mu \int_{x_0}^{x} \phi(s) \, ds \right). \tag{12}$$

The most used growth rate for trees is the classical Richards growth equation (Richards, 1959):

$$g(x) = ax \left(1 - \left(\frac{x}{x_M} \right)^b \right). \tag{13}$$

When $b = 1$ the Richards equation matches the logistic equation; parameter b allows the shape of the upper part of the curve (sigmoid curve), to be independent of the shape of the lower part. When $b > 1$ the maximum slope of the curve is attained for $x > x_M/2$ and when $b < 1$ for $x < x_M/2$. The time required for a tree to increase d.b.h. from x_0 to x assuming Richards growth law is

$$\varphi(x) = \frac{1}{ab} \ln \left(\frac{x^b(x_M^b - x_0^b)}{x_0^b(x_M^b - x^b)} \right) \tag{14}$$

and the stable d.b.h. distribution is

$$u^*(x) = \frac{Rx_M^b}{ax(x_M^b - x^b)} \left(\frac{x^b(x_M^b - x_0^b)}{x_0^b(x_M^b - x^b)} \right)^{-\mu/ab}. \tag{15}$$

This distribution presents an inverse J-shaped form for large enough mortality rate; to be precise, if $\mu > ab$, see (Fig. 1(a)). Otherwise, that is $\mu \leqslant ab$ there is an effect of accumulation of trees with d.b.h. close to the maximum size which yields an U-shaped form (Fig. 1(b)).

A different type of equilibrium curve which is frequently observed in the field is the unimodal one. We propose the following family of growing rates, that includes Richards' ones ($c = 0$), which give unimodal equilibrium distributions for certain parameters values (Fig. 1(c)).

$$g(x) = ax \left(1 - \left(\frac{x}{x_M} \right)^b \right) \exp(-cx). \tag{16}$$

3.2. Light competition and stand structure

We introduce the light competition in the model by separately incorporating shade intolerance effects on growth, mortality and recruitment.

3.2.1. Light-dependent tree growth and stand structure

We assume now that the recruitment rate, R, and the mortality rate, μ, are constant. The growth rate is dependent on light competition in the following way:

$$G(x, B(x, t)) = g(x)H(B(x, t)), \tag{17}$$

where $H(z)$ is a decreasing function with values in $(0, 1]$. Then system (3)–(5) reads as follows:

$$u_t(x, t) + (G(x, B(x, t))u(x, t))_x$$
$$= -\mu u(x, t) \quad (x_0 < x < x_M, \ t > 0), \tag{18}$$

$$G(x_0, B(x_0, t))u(x_0, t) = R \quad (t > 0), \tag{19}$$

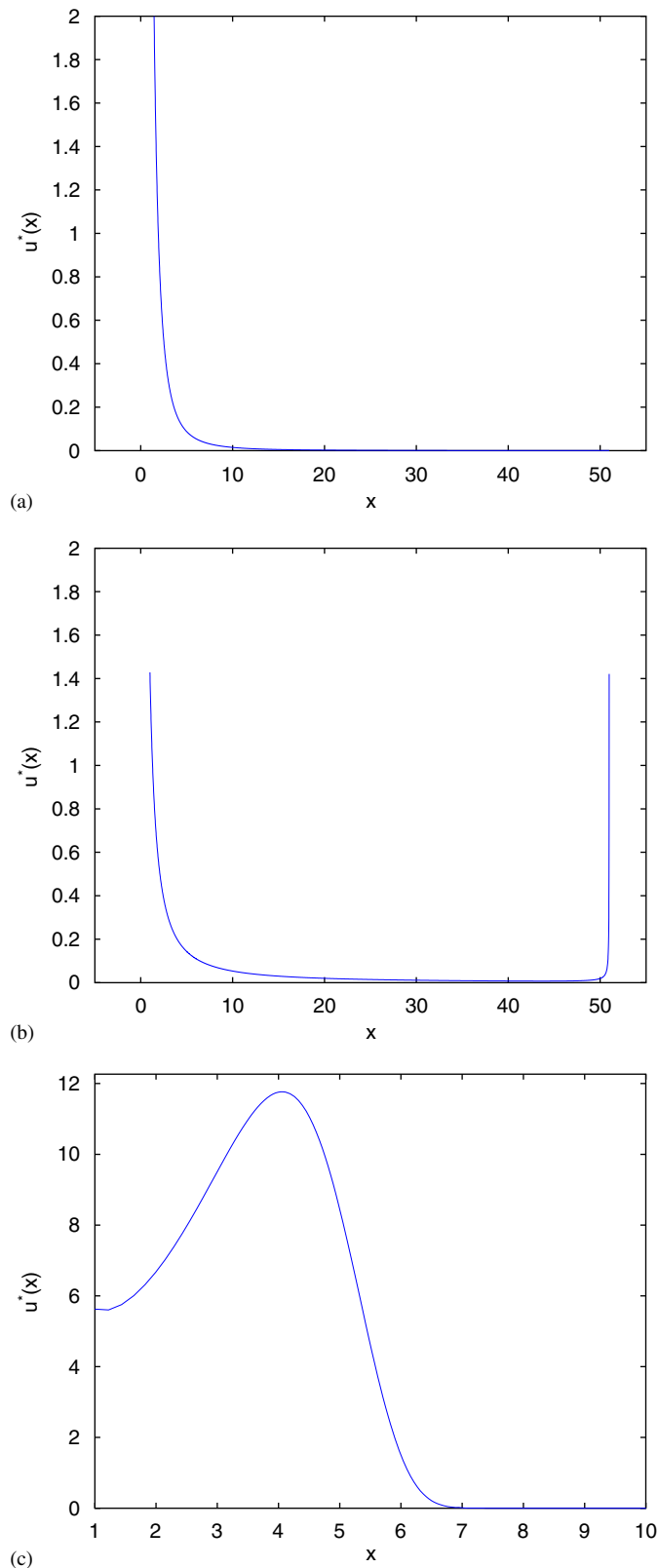$$u(x, 0) = u_0(x) \quad (x_0 \leqslant x \leqslant x_M). \tag{20}$$

(a)

(b)

(c)

Fig. 1. Stable distribution curve for parameter values: (a) $a = 7$, $b = 16$, $\mu = 3$; (b) $a = 2$, $b = 1$, $\mu = 3$; (c) $a = 2$, $b = 1$, $c = 1$, $\mu = 0.1$.

This kind of system is a particular case, under some technical assumptions, of the system studied in Kraev (2001), where it is proved the existence and unicity of its solution.

The steady state solution, $u^*(x)$, of system (18)–(19) must verify the following equation:

$$(G(x, B^*(x))u^*(x))_x = -\mu u^*(x) \quad (x_0 < x < x_M), \tag{21}$$

where $B^*(x) = \int_x^{x_M}(\pi/4)\sigma^2 u^*(\sigma)\,d\sigma$. Even though it is not possible to solve explicitly Eq. (21) we can obtain in some cases the shape of $u^*(x)$ through its derivative which satisfies the following equation:

$$\frac{d}{dx}u^*(x) = -\left(\frac{d}{dx}(G(x, B^*(x))) + \mu\right)\frac{u^*(x)}{G(x, B^*(x))}$$

$$= -\left(g'(x)H(B^*(x)) + g(x)H'(B^*(x))\right)$$

$$\times\left(-\frac{\pi}{4}x^2 u^*(x)\right) + \mu\right)\frac{u^*(x)}{G(x, B^*(x))}. \tag{22}$$

If we do not consider light competition but we keep the same individual growth rate $g(x)$ the derivative of the stable distribution simplifies to

$$-(g'(x) + \mu)u^*(x)/g(x).$$

The sign of this expression depends on the term $g'(x) + \mu$; for the x for which it is positive (negative) the stable distribution is decreasing (increasing). Having in mind that

$$g(x)H'(B^*(x))\left(-\frac{\pi}{4}x^2 u^*(x)\right) > 0 \quad \text{and} \quad H(B^*(x)) \leqslant 1$$

it is straightforward to see that $g'(x) + \mu > 0$ implies that

$$g'(x)H(B^*(x)) + g(x)H'(B^*(x))\left(-\frac{\pi}{4}x^2 u^*(x)\right) + \mu > 0,$$

that is, if the stable distribution without light competition is decreasing on an interval of values of x the same happens with the steady state solution $u^*(x)$ in the case of light competition on growing. In particular, if $g(x)$ without light competition yields an inverse J-shaped stable distribution curve we obtain a decreasing curve when adding light competition in the way described in (17).

3.2.2. Light-dependent tree mortality and stand structure

We suppose now that light competition is preferentially acting on mortality rather than growth. We assume that the recruitment rate is a constant R and the growing rate is a function $g(x)$ independent of $B(x, t)$. The mortality rate is dependent on light competition in the following way:

$$M(x, B(x, t)) = \mu + K(B(x, t)), \tag{23}$$

where $K(z)$ is a nonnegative increasing function. System (3)–(5) reads in this case as follows:

$$u_t(x, t) + (g(x)u(x, t))_x$$
$$= -M(x, B(x, t))u(x, t) \quad (x_0 < x < x_M,\ t > 0), \tag{24}$$

$$g(x_0)u(x_0, t) = R \quad (t > 0), \tag{25}$$

$$u(x, 0) = u_0(x) \quad (x_0 \leqslant x \leqslant x_M) \tag{26}$$

and it is still in the frame of Kraev (2001). The steady state solution, $u^*(x)$, of system (24)–(25) must verify the

following equation:

$$(g(x)u^*(x))_x = -M(x, B^*(x))u^*(x) \quad (x_0 < x < x_M) \qquad (27)$$

and its derivative satisfies

$$\frac{d}{dx} u^*(x) = -(g'(x) + M(x, B^*(x)))\frac{u^*(x)}{g(x)}$$

$$= -(g'(x) + \mu + K(B^*(x)))\frac{u^*(x)}{g(x)}. \qquad (28)$$

This expression allow us to do an analysis of the form of the stable distribution analogous to the one did in the previous case where light competition affected growing. It is straightforward to see that $g'(x) + \mu > 0$ implies that $(d/dx)u^*(x) > 0$ and so we still have that on the intervals where, without light competition, the stable distribution is decreasing $u^*(x)$ is also decreasing. In particular, inverse J-shaped stable distributions still keep decreasing by adding light competition in the way described in (23).

3.2.3. Recruitment suppression and stand structure and dynamics

We represent recruitment suppression (e.g. by means of shade intolerance at the sapling stage) by taking a zero recruitment rate, $R = 0$. If we also assume a growth rate, $g(x)$, independent of light competition and a constant mortality rate μ, we are considering a particular case of system (6)–(8) in which solution is

$$u(x,t) = \begin{cases} u_0(\varphi^{-1}(\varphi(x) - t))e^{-\mu t}\dfrac{g(\varphi^{-1}(\varphi(x) - t))}{g(x)} & \text{if } \varphi(x) > t, \\ 0 & \text{if } \varphi(x) < t. \end{cases}$$

$$(29)$$

Taking $g(x) = 2x(1 - (x/51)^{0.05})$, $x_0 = 1$, $x_M = 51$, $\mu = 0.1$ and the initial condition $u_0(x)$ described in Appendix B for the case of $R = 0$, we see in Fig. 2(a) the evolution of $u(x,t)$ by showing it at 17 uniformly distributed times $t = 0, 6.25, 12.50, \ldots, 87.50, 93.75, 100$.

In Figs. 2(b) and (c) the same kind of representation is done for two cases with the same characteristic as the previous example but including light competition on growing with different strength.

Fig. 2(b) corresponds to the growth rate

$$G(x, B(x,t)) = 2x(1 - (x/51)^{0.05})10^{-3} \exp(-B(x,t))$$

and Fig. 2(c) to

$$G(x, B(x,t)) = 2x(1 - (x/51)^{0.05})10^{-2} \exp(-B(x,t)).$$

4. Discussion

Patterns of stand structure and dynamics result from a combination of several factors such as disturbance history, species physiology, competition as well as site ecological conditions (Oliver and Larson, 1990; Lorimer and Krug, 1983; Abrams and Downs, 1990). Given the dynamic nature of population interaction and the number of factors involved, identification of the mechanisms underlying
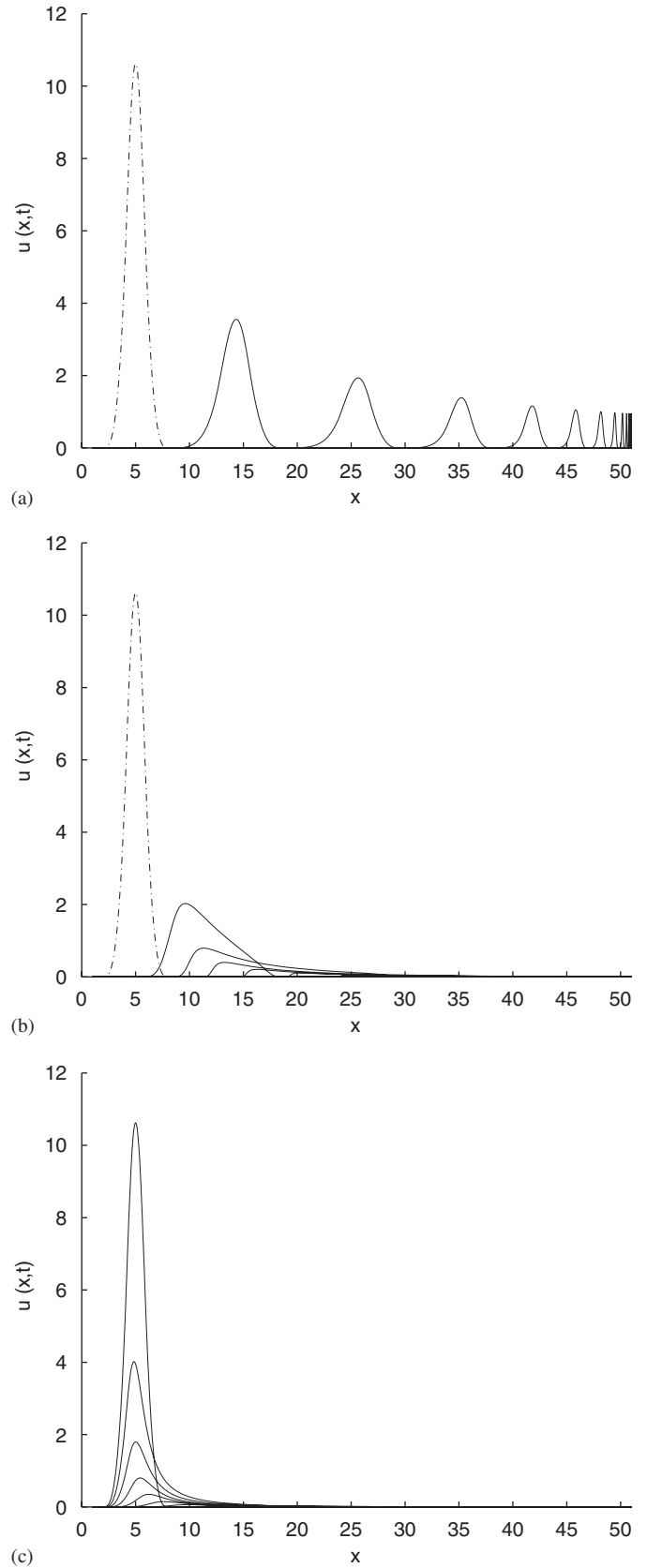

Fig. 2. Population d.b.h. distribution at 17 different times ($t = 0, 6.25, 12.50, \ldots, 87.50, 93.75, 100$) for parameter values $a = 2$, $b = 0.05$, $\mu = 0.1$, $R = 0$ and: (a) $H(z) = 1$ (no light competition); (b) $H(z) = 10^{-3}e^{-z}$; (c) $H(z) = 10^{-2}e^{-z}$.

stand structure cannot be easily grasped through experimental studies and it is best achieved through dynamic models that connect tree individual performance to stand level properties (Kohyama, 1991a; Hara and Yokozawa, 1994).

Contrary with classical silvicultural theory (Lanier, 1986) and observational models (Lorimer and Krug, 1983) our results do not show evidence of a causal relationship between shade tolerance and stand structure which converged towards an inverse J-shaped curve under a wide range of light-dependent growth and mortality conditions. In contrast realistic patterns in stand dynamics for shade intolerant species were only obtained when recruitment was completely suppressed (Fig. 2(b)). This suggests that juvenile stages may have a disproportionate effect on final stand structure and composition relative to competition at later stages (Kobe et al., 1995; Pacala et al., 1996).

Predicted patterns on transient stand dynamics in populations regulated by one-sided competition and null recruitment did match the classical silvicultural model of stand dynamics (e.g. Lanier, 1986, Fig. 2(b)). This agreement is based on the travelling of the diameter distribution, positive skewness and a gradually flattening shape previously reported. Positive skewness in diameter distributions when no competitive interactions take place have been reported by Hara (1984b), while positive skewness has been described in tree populations structured by light competition (Lieffers, 1986; Agren and Zackrisson, 1990). Our results also agree with observed dynamics of ramet populations within a stool which is also regarded as a system structured by one-sided competition (Ford and Newbould, 1970). Specifically observed changes in stand structure patterns of Quercus ilex managed by selection thinning over a 30 year period (Retana et al., 1992) show similar trends than our model predictions including negative skewness and gradual progression towards an unimodal distribution.

Interestingly the two main type of equilibrium curves observed in the field can result from differences in the growth-size dependence function (rate of growth decline with respect to size) and even in the absence of competition. This finding suggests the need to examine other physiological size-dependent processes that can have a greater impact on long term population structure, including allometric relations (Hara and Yokozawa, 1994). Altogether different plant traits are likely to be correlated, defining species specific strategic such as r-like species that experience both a faster decline in growth rates with respect to size and shade intolerance, or K-like species with more conservative metabolism and greater tolerance of shade. Suites of traits associated with a given selective pressure can be under genetic control (Chapin et al., 1993) or result from tradeoffs among traits (Tilman, 1988).

Further understanding of the mechanisms leading to a given diameter distribution shape should also take into consideration disparity of ecological site conditions that can influence growth rates as well as interspecific competitive relationships. For example a variety of stand structure curves have been reported for the same species along an environmental gradient (Parker, 1984; Butson et al., 1987) or depending on whether stands were mixed or monospecific (Lorimer and Krug, 1983).

Over the last decades a number of empirical and simulation studies have been key for increasing our understanding of the mechanisms underlying forest structure. Previous models aiming to understand changes in stand structure in terms of species individual ecology have typically relied on individual-based simulations that trace the fate of each individual tree through its biological cycle (Shugart, 1984; Tilman, 1988). Analytical models of stand dynamics by means of PDE allow us to connect stand level patterns to in individual tree performance and to accommodate a wide range of diameter distributions in terms of a few biologically interpretable parameters. Also they are preferred to simulations because of increases in computing speed (Lischke et al., 1998). Aggregated and analytical models are of greater heuristic interest as can be analyzed for some particular cases.

Development of a general theory of stand dynamics will require advances in several fronts. First, in our study the definition of forest stand implies a patch size small enough so trees within the stand interact with same strength regardless of the distance among them. Tree competition, however, is rather a neighborhood process (sensu Pacala et al., 1996) in which emergent or aggregated collective forest properties such as production may depend critically on local individual interactions (Pacala and Deutschman, 1995; Levin and Pacala, 1997). Therefore, our results can only be extrapolated to small stands. Secondly plants are plastic and can change their allometry in response to resource variability, with these changes having a critical impact on stand structure (Hara and Yokozawa, 1994). Third, many of the processes involved in forest dynamics are stochastic and predictability seems only possible at certain scales. Understanding how local stochastic processes scale up to the stand and forest level as deterministic processes seems key in order to provide a realistic description of system dynamics (Lischke et al., 1998). Therefore, the challenge remains to keep model complexity at its minimum but still gradually include critical biological detail such as plasticity, stochasticity and spatial interactions that are essential components of forest stand dynamics.

Acknowledgments

Appendix A. Numerical method

In this section we describe a method which integrates numerically Eqs. (3)–(5) along the characteristic curves and uses the composite trapezoidal quadrature rule to approximate the nonlocal terms. Also, this scheme employs a selection procedure, at each time level, that avoids an increment on the number of nodes. We begin rewriting the partial integro-differential equation in a more suitable form for its numerical treatment. So we define

$$m(x, z, u) = \mu(x, z) + g_x(x, z) - g_z(x, z)\gamma(x)u,$$

where $\gamma(x) = (\pi/4)x^2$, thus (3) has the form

$$u_t(x, t) + g(x, B(x, t)) u_x(x, t)$$
$$= -m(x, B(x, t), u(x, t))u(x, t), \tag{30}$$

$x_0 < x < x_M$, $t > 0$. Next, we denote by $x(t; t^*, x^*)$ the characteristic curve of Eq. (30) that takes the value x^* at time t^*. This is the solution of the next initial value problem

$$\begin{cases} x'(t; t^*, x^*) = g(x(t; t^*, x^*), B(x(t; t^*, x^*), t)), & t \geqslant t^*, \\ x(t^*; t^*, x^*) = x^*. \end{cases} \tag{31}$$

Note that $x(t; 0, x_M) = x_M$, $t \geqslant 0$; because we are assuming that $g(x_M, z) = 0$. Then, we define the function

$$w(t; t^*, x^*) = u(x(t; t^*, x^*), t), \quad t \geqslant t^*, \tag{32}$$

that satisfies the next initial value problem

$$\begin{cases} \dfrac{\mathrm{d}}{\mathrm{d}t} w(t; t^*, x^*) = -m(x(t; t^*, x^*), B(x(t; t^*, x^*), t), \\ \qquad w(t; t^*, x^*))w(t; t^*, x^*), \qquad t \geqslant t^*, \\ w(t^*; t^*, x^*) = u(x^*, t^*), \end{cases} \tag{33}$$

and therefore, it can be represented with the next formula

$$w(t; t^*, x^*) = u(x^*, t^*) \exp\left\{-\int_{t^*}^{t} m(x(\tau; t^*, x^*),\right.$$
$$\left. B(x(\tau; t^*, x^*), \tau), w(\tau; t^*, x^*)) \, \mathrm{d}\tau \right\}. \tag{34}$$

(Recall that $B(x, t)$ is defined by (1).) We suppose that $u(x_M, 0) = 0$ and then $u(x_M, t) = 0$, $t \geqslant 0$. We shall use this property in our numerical method. However, it can be easily modified to cover other cases.

Let J and N be positive integers, we define the spatial and time discretization parameters as $h = (x_M - x_0)/J$ and $k = T/N$, respectively. The discrete time levels are $t_n = nk$, $0 \leqslant n \leqslant N$, and the initial grid nodes are $X_j^0 = jh$, $0 \leqslant j \leqslant J$. We suppose that the approximations to the theoretical solution in such nodes are known, U_j^0, $0 \leqslant j \leqslant J$. Thus,

we denote

$$\mathbf{X}^0 = \{X_0^0 = x_0, X_1^0, \ldots, X_{J-1}^0, X_J^0 = x_M\},$$
$$\mathbf{U}^0 = \{U_0^0, U_1^0, \ldots, U_{J-1}^0, U_J^0 = 0\}.$$

Also we introduce $\mathbf{I}^0 = \{I_0^0, I_1^0, \ldots, I_{J-1}^0, I_J^0 = 0\}$, where

$$I_j^0 = Q_j^0(\mathbf{X}, \gamma(\mathbf{X})\mathbf{U}), \tag{35}$$

is defined as the discrete version of (1) at $x = X_j^0$, $j = 0, 1, \ldots, J$.

We will obtain the numerical approximations at the time level t_1 as follows: first we define the grid nodes $\mathbf{X}^1 = \{X_0^1 = x_0, X_1^1, \ldots, X_J^1, X_{J+1}^1 = x_M\}$, by the numerical integration of (31)

$$X_{j+1}^1 = X_j^0 + k \, g(X_{j+1}^{1/2}, I_{j+1}^{1/2}), \quad 0 \leqslant j \leqslant J-1. \tag{36}$$

Then we calculate the corresponding approximations to the theoretical solution $\mathbf{U}^1 = \{U_0^1, U_1^1, \ldots, U_J^1, U_{J+1}^1 = 0\}$, by means of the following discretization of (34):

$$U_{j+1}^1 = U_j^0 \exp(-km(X_{j+1}^{1/2}, I_{j+1}^{1/2}, U_{j+1}^{1/2})),$$
$$0 \leqslant j \leqslant J-1. \tag{37}$$

Finally, we derive the approximation U_0^1 to $u(x_0, t_1)$ from a discrete version of the boundary condition (4)

$$U_0^1 = \frac{I_0^1 r(I_0^1)}{g(x_0, I_0^1)}, \tag{38}$$

where

$$X_0^{1/2} = x_0, \quad X_{j+1}^{1/2} = X_j^0 + \frac{k}{2} g(X_j^0, I_j^0),$$
$$0 \leqslant j \leqslant J-1, \quad X_{J+1}^{1/2} = x_M,$$

$$U_{j+1}^{1/2} = U_j^0 \exp\left(-\frac{k}{2} m(X_j^0, I_j^0, U_j^0)\right),$$
$$0 \leqslant j \leqslant J-1, \quad U_{J+1}^{1/2} = 0,$$

and we define

$$I_j^{1/2} = Q_j^{1/2}(\mathbf{X}, \gamma(\mathbf{X})\,\mathbf{U}), \quad 1 \leqslant j \leqslant J+1,$$
$$I_j^1 = Q_j^1(\mathbf{X}, \gamma(\mathbf{X})\,\mathbf{U}), \quad 0 \leqslant j \leqslant J+1,$$

$$Q_j^s(\mathbf{X}, \mathbf{V}) = \sum_{l=j}^{J+1} \frac{X_{l+1}^s - X_l^s}{2} (V_l^s + V_{l+1}^s),$$

$$0 \leqslant j \leqslant J+1, \quad s = \frac{1}{2}, 1.$$

We observe that, at consecutive time levels, we are working with a different number of nodes because we have introduced a new node that fluxes through the boundary. So, at the time level t_n we have $(J+1)$ grid nodes, and at time level t_{n+1} we have $(J+2)$ but we want to keep constant the number of nodes not to increase the computational cost. Therefore we select one characteristic curve and we do not compute the approximations at such curve. Then, we eliminate the first grid node X_l^1

that satisfies

$$|X^1_{l+1} - X^1_{l-1}| = \min_{1 \leqslant j \leqslant J} |X^1_{j+1} - X^1_{j-1}|, \tag{39}$$

and the corresponding value in the vectors $\mathbf{U}^1$ and $\mathbf{I}^1$.

Next, we describe the general time step t_{n+1}, $0 \leqslant n \leqslant N - 1$. Now, we suppose that the numerical approximations at the previous time level t_n are known

$$\{X^n_0 = x_0, X^n_1, \ldots, X^n_{J-1}, X^n_J = x_M\},$$
$$\{U^n_0, U^n_1, \ldots, U^n_{J-1}, U^n_J = 0\},$$

and $\{I^n_0, I^n_1, \ldots, I^n_{J-1}, I^n_J\}$. We recall that X^n_j and X^{n+1}_j, $0 \leqslant j \leqslant J - 1$, are (numerically) in the same characteristic curve. First, we compute the grid values at the time level t_{n+1},

$$\mathbf{X}^{n+1} = \{X^{n+1}_0 = x_0, X^{n+1}_1, \ldots, X^{n+1}_J, X^{n+1}_{J+1} = x_M\},$$

by means of the numerical integration of (31)

$$X^{n+1}_{j+1} = X^n_j + k\, g(X^{n+1/2}_{j+1}, I^{n+1/2}_{j+1}), \quad 0 \leqslant j \leqslant J - 1, \tag{40}$$

and the approximations to the theoretical solution in these nodes at such time level

$$\mathbf{U}^{n+1} = \{U^{n+1}_0, U^{n+1}_1, \ldots, U^{n+1}_J, U^{n+1}_{J+1} = 0\},$$

using the discretization of (34)

$$U^{n+1}_{j+1} = U^n_j \exp(-km(X^{n+1/2}_{j+1}, I^{n+1/2}_{j+1}, U^{n+1/2}_{j+1})),$$
$$0 \leqslant j \leqslant J - 1.$$

We complete the equations at the time level t_{n+1} with the approximation U^{n+1}_0 to $u(x_0, t_{n+1})$ using a discretization of the boundary condition (4)

$$U^{n+1}_0 = \frac{I^{n+1}_0 (I^{n+1}_0)}{g(x_0, I^{n+1}_0)}, \tag{41}$$

where

$$X^{n+1/2}_0 = x_0, \quad X^{n+1/2}_{j+1} = X^n_j + \frac{k}{2} g(X^n_j, I^n_j),$$
$$0 \leqslant j \leqslant J - 1, \ X^{n+1/2}_{J+1} = x_M,$$

$$U^{n+1/2}_{j+1} = U^n_j \exp\left(-\frac{k}{2} m(X^n_j, I^n_j, U^n_j)\right),$$
$$0 \leqslant j \leqslant J - 1, \quad U^{n+1/2}_{J+1} = 0,$$

and we define

$$I^{n+1/2}_j = Q^{n+1/2}_j(\mathbf{X}, \gamma(\mathbf{X})\,\mathbf{U}), \quad 1 \leqslant j \leqslant J + 1,$$
$$I^{n+1}_j = Q^{n+1}_j(\mathbf{X}, \gamma(\mathbf{X})\,\mathbf{U}), \quad 0 \leqslant j \leqslant J + 1,$$
$$Q^s_j(\mathbf{X}, \mathbf{V}) = \sum_{l=j}^{J+1} \frac{X^s_{l+1} - X^s_l}{2}(V^s_l + V^s_{l+1}),$$
$$s = n + \frac{1}{2}, n + 1.$$

Now, we have $J + 2$ nodes at the time level t_{n+1} and we want to keep constant the number of nodes therefore we select one characteristic curve and we do not compute the approximations at such curve. Then, we eliminate the first grid node X^{n+1}_l that satisfies

$$|X^{n+1}_{l+1} - X^{n+1}_{l-1}| = \min_{1 \leqslant j \leqslant J} |X^{n+1}_{j+1} - X^{n+1}_{j-1}|, \tag{42}$$

and the corresponding value in the vectors $\mathbf{U}_{n+1}$ and $\mathbf{I}_{n+1}$.

Appendix B. Simulations conditions

In all simulations performed we used parameters values $x_0 = 1$ and $x_M = 51$ for minimum and maximum d.b.h. sizes, the initial and final times are, respectively, $t = 0$ and $t_f = 100$. Dynamics of stand structure shown in Fig. 2 correspond to 17 uniformly distributed times $t = 0, 6.25, 12.50, \ldots, 87.50, 93.75, 100$.

Simulations reported in this study depart from young even-aged populations. For the initial and boundary conditions to be mathematically consistent it is required that the constant recruitment rate verifies $R(t) = R = g(x_0, B(x_0, 0))u_0(x_0)$ and so we need to distinguish in the recruitment law among cases with and without recruitment. Initial d.b.h. distribution for the case with positive constant recruitment is an asymmetric unimodal curve defined in the following form for technical reasons related to the numerical method (Fig. 3):
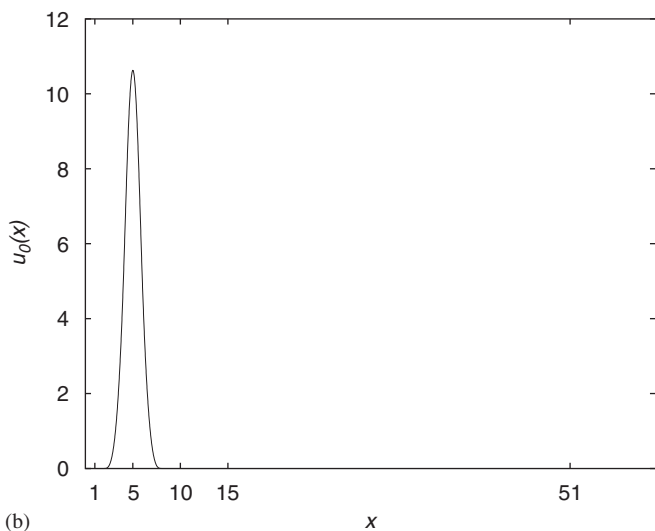
$$u_0(x) = \begin{cases} 5 + 5\left(\dfrac{x-2}{2} + 1\right)^3, & x \leqslant 2, \\[2mm] 10 + 15\dfrac{x-2}{2}\left(1 + \dfrac{x-2}{2}\right) + 30\left(\dfrac{x-2}{2}\right)^3\left(\dfrac{x-2}{2} - 2\right), & 2 < x \leqslant 4, \\[2mm] 5\left(2 - \dfrac{x-2}{2}\right)^3\left(2 + 3\left(\dfrac{x-2}{2} - 1\right)\left(1 + 2\left(\dfrac{x-2}{2} - 1\right)\right)\right), & 4 < x \leqslant 6, \\[2mm] 0 & x > 6. \end{cases} \tag{43}$$

The corresponding initial distribution for the case without recruitment is represented by a symmetric unimodal curve (Fig. 3) defined as

$$u_0(x) = \begin{cases} 0, & x \leqslant 2, \\ 5\left(\dfrac{x-4}{2}+1\right)^3, & 2 \leqslant x \leqslant 4, \\ 5\left(1+3\dfrac{x-4}{2}\left(1+\dfrac{x-4}{2}\right)+6\left(\dfrac{x-4}{2}\right)^3\left(\dfrac{x-4}{2}-2\right)\right), & 4 < x \leqslant 6, \\ 5\left(2-\dfrac{x-4}{2}\right)^3, & 6 < x \leqslant 8, \\ 0, & x > 8. \end{cases} \qquad (44)$$
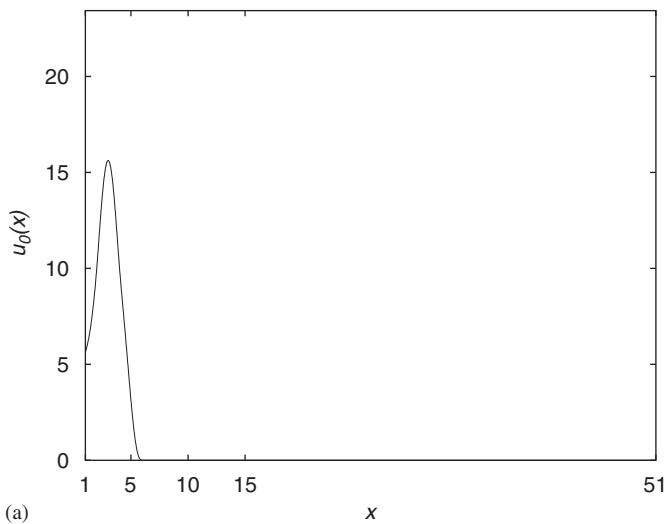
Fig. 3. Initial d.b.h. distribution for: (a) constant non-zero recruitment; (b) zero recruitment.

References

Abia, L.M., Angulo, O., López-Marcos, J.C., 2004. Size-structured population dynamics models and their numerical solutions. Discrete Contin. Dyn. Syst. B 4, 1203–1222.

Abia, L.M., Angulo, O., López-Marcos, J.C., 2005. Age-structured population models and their numerical solution. Ecol. Modelling 188, 112–136.

Abrams, M., Downs, J.A., 1990. Successional replacement of old-growth white oak by mixed mesophytic hardwoods in southwestern Pennsylvania. Can. J. For. Res. 20, 1864–1870.

Agren, J., Zackrisson, O., 1990. Age and size structure of Pinus sylvestris populations on mires in central and northern Sweden. J. Ecol. 78, 1049–1062.

Angulo, O., López-Marcos, J.C., 1999. Numerical schemes for size-structured population equations. Math. Biosci. 157, 169–188.

Angulo, O., López-Marcos, J.C., 2000. Numerical integration of nonlinear size-structured population equations. Ecol. Modelling 133, 3–14.

Angulo, O., López-Marcos, J.C., 2002. Numerical integration of autonomous and no autonomous nonlinear size-structured population models. Math. Biosci. 177–178, 39–71.

Angulo, O., López-Marcos, J.C., 2004. Numerical integration of fully nonlinear size-structured population models. Appl. Numer. Math. 50, 291–327.

Angulo, O., Durán, A., López-Marcos, J.C., 2005. A numerical simulation for the dynamics of the sexual phase of monogonont rotifera. C. R. Biologies 327, 293–303.

Assman, E., 1970. The principles of forest yield study. Trans. S.H. Gardiner. Pergamon, Oxford.

Bailey, R.L., Dell, T.R., 1973. Quantifying diameter distributions with the Weibull function. For. Sci. 19, 97–104.

Bees, M.A., Angulo, O., López-Marcos, J.C., Schley, D., 2006. Dynamics of a structured slug population model in the absence of seasonal variation. Math. Mod. Meth. Appl. Sci. 12 (16).

Binkley, D., Stape, J.L., Ryan, M.G., Barnard, H.R., Fownes, J., 2002. Age-related decline in forest ecosystem growth: an individual tree, stand structure hypothesis. Ecosystems 5, 58–67.

Butson, R.G., Knowles, P., Farmer Jr., R.E., 1987. Age and size structure of marginal disjunct populations of Pinus resinosa. J. Ecol. 75, 685–692.

Calsina, À., Saldaña, J., 1997. Asymptotic behaviour of a model of hierarchically structured population dynamics. J. Math. Biol. 35, 967–987.

Canham, C.D., 1989. Different responses to gaps among shade-tolerant tree species. Ecology 70, 548–550.

Casagrandi, R., Rinaldi, S., 1999. A minimal model for forest fire regimes. Am. Nat. 153, 527–539.

Chapin III, F.S., Autumn, K., Pugnaire, F., 1993. Evolution of suites of traits in response to environmental stress. Am. Nat. 142, S78–S92.

Crawley, M.J., (Ed.) 1986. Plant Ecology. Blackwell Scientific Press, Oxford.

Cushing, J.M., 1998. An Introduction to Structured Population Dynamics. CBMS-NSF Regional Conference Series in Applied Mathematics, vol. 71. SIAM, Philadelphia.

De Roos, A.M., 1997. A gentle introduction to physiologically structured population models. In: Tuljapurkar, S., Caswell, H. (Eds.), Structured-

Population Models in Marine, Terrestrial, and Freshwater Systems. Chapman & Hall, New York, pp. 119–204.

Dercole, F., Niklas, K., Rand, R., 2005. Self-thinning and community persistence in a simple size-structured dynamical model of plant growth. J. Math. Biol. 51, 333–354.

Espelta, J.M., Riba, M., Retana, J., 1995. Patterns of seedling recruitment in West Mediterranean coppiced holm-oak (Quercus ilex L.) forests as influenced by canopy development. J. Veg. Sci. 6, 645–672.

Ford, E.D., Newbould, P.J., 1970. Stand structure and dry weight production through the sweet chestnut (Castanea sativa) coppice cycle. J. Ecol. 58, 275–296.

Glitzenstein, J.S., Harcombe, P.A., Streng, D.R., 1986. Disturbance, succession and maintenance of species diversity in an east Texas forest. Ecol. Monogr. 56, 243–258.

Gurtin, M.E., MacCamy, R.C., 1974. Nonlinear age-dependent population dynamics. Arch. Rat. Mech. Anal. 54, 281–300.

Hara, T., 1984a. A stochastic model and the moment dynamics of the growth and size distribution in plant populations. J. Theor. Biol. 109, 173–190.

Hara, T., 1984b. Dynamics of stand structure in plant monocultures. J. Theor. Biol. 110, 223–239.

Hara, T., 1985. A model for mortality in a self-thinning plant population. Ann. Botany 55, 667–675.

Hara, T., 1992. Effects of the mode of competition on stationary size distribution in plant populations. Ann. Bot. 69, 509–513.

Hara, T., Yokozawa, M., 1994. Effects of physiological and environmental variations on size-structure dynamics in plant populations. Ann. Bot. 73, 39–51.

Harper, J.L., 1977. Population Biology of Plants. Academic Press, New York.

Hubbell, S.P., 1980. Seed predation and the coexistence of tree species in tropical forests. Oikos 35, 214–229.

Hurtt, G.C., Pacala, S.W., 1995. The consequences of recruitment limitation: reconciling chance, history and competitive differences between plants. J. Theor. Biol. 176, 1–12.

Iannelli, M., 1994. Mathematical Theory of Age-Structured Populations Dynamics. Giardini Editori e Stampatori, Pisa.

Kermack, W., McKendrick, A., 1933. Contributions to the mathematical theory of epidemics III. Further studies on the problem of endemicity. Proc. R. Soc. 141, 94–122.

Keyfitz, N., 1968. Introduction to the Mathematics of Population. Addison Wesley, Reading, MA.

Knox, R.G., Peet, R.K., Christensen, N.L., 1989. Population dynamics in loblolly pine stands: changes in skewness and size inequality. Ecology 70, 1153–1166.

Kobe, R.K., Pacala, S.W., Silander Jr., J.A., Canham, C.D., 1995. Juvenile tree survivorship as a component of shade tolerance. Ecol. Appl. 5, 517–532.

Kohyama, T., 1991a. Simulation of the structural development of warm-temperate rain forest stands. Ann. Bot. 63, 625–634.

Kohyama, T., 1991b. Simulating stationary size distribution of trees in rain forests. Ann. Bot. 68, 173–180.

Kohyama, T., 1992. Size-structured multi-species model of rain forest trees. Funct. Ecol. 6, 206–212.

Kraev, E.A., 2001. Existence and uniqueness for height structured hierarchical population models. Nat. Resour. Modelling 14, 45–70.

Lanier, L., 1986. Précis de Sylviculture. ENGREF. Nancy.

Levin, S.A., Pacala, S.W., 1997. Theories of simplification and scaling of spatially distributed processes. In: Tilman, D., Kareiva, P. (Eds.), Spatial Ecology: The Role of Space in Population Dynamics and Interspecific Interactions. Princeton University Press, Princeton, NJ, pp. 271–296.

Lieffers, V.J., 1986. Stand structure variability in growth and intraspecific competition in a peatland stand of black spruce Picea mariana. Holarc. Ecol. 9, 58–64.

Liocurt, F.de, 1898. De l'aménagement des sapinières. Soc. For. Franche-Comté Belfort Bull. 6, 369–405.

Lischke, H., 2001. New developments in forest modelling: convergence between applied and theoretical approaches. Nat. Resour. Modeling 14, 71–102.

Lischke, H., Löffler, T.J., Fischlin, A., 1998. Aggregation of individual trees and patches in forest succession models: capturing variability with height structured, random, spatial distributions. Theor. Popul. Biol. 54, 213–226.

Lookingbill, T., Zavala, M.A., 2000. Spatial pattern of holm oak (Quercus ilex) and downy oak (Quercus pubescens) recruitment in Aleppo pine (Pinus halepensis) dominated woodlands. J. Veg. Sci. 11, 607–612.

Lorimer, C.G., 1980. Age structure and disturbance history of a southern Appalachian virgin forest. Ecology 61, 1169–1184.

Lorimer, C.G., Krug, A.G., 1983. Diameter distributions in even-aged stands of shade-tolerant and mid-tolerant and midtolerant tree species. Am. Mid. Nat. 109, 331–345.

Metz, J.A.J., Diekmann O., 1986. The Dynamics of Physiologically Structured Populations. Lecture Notes in Biomathematics, vol. 68. Springer, Berlin.

Nagano, M., 1978. Dynamics of stand development. In: Kira, T., Ono, Y., Osokawa, T. (Eds.), Biological Production in a Warm-Temperate Evergreen Oak Forest of Japan, vol. 18. University of Tokyo Press, JIBP Synthesis Edition, pp. 21–31.

Oliver, C.D., Larson, B.C., 1990. Forest Stand Dynamics. McGraw-Hill, New York.

Pacala, S.W., Deutschman, D., 1995. Details that matter: the spatial distribution of individual trees maintains forest ecosystem function. Oikos 74, 357–365.

Pacala, S.W., Canham, C.D., Saponara, J., Silander, J.A., Kobe, R.K., Ribbens, E., 1996. Forest models defined by field measurements: estimation, error analysis and dynamics. Ecol. Monogr. 66, 1–43.

Parker, A.J., 1984. Stand structure in subalpine forests of Yosemite National Park. California. For. Sci. 34, 1047–1058.

Retana, J., Riba, M., Castell, C., Espelta, J.M., 1992. Regeneration by sprouting of holm-oak (Quercus ilex) stands exploited by selection thinning. Vegetation 99–100, 355–364.

Richards, F.J., 1959. A flexible growth function for empirical use. J. Exp. Bot. 10, 290–300.

Shinko, J.W., Streifer, W., 1967. A new model for age-size structure of a population. Ecology 48, 910–918.

Shugart, H.H., 1984. A Theory of Forest Dynamics: the Ecological Implications of Forest Succession Models. Springer, Berlin.

Smith, D.M., 1962. The Practice of Silviculture. Wiley, New York.

Sulsky, D., 1994. Numerical solution of structured population models ii: mass structure. J. Math. Biol. 32, 491–514.

Takada, T., Iwasa, Y., 1986. Size distribution dynamics of plants with interaction by shading. Ecol. Modelling 33, 173–184.

Tilman, D., 1988. Plant strategies and the dynamics and structure of plant communities. Princeton University Press, Princeton, NJ.

Tucker, S., Zimmerman, S., 1988. A nonlinear model of population-dynamics containing and arbitrary number of continuous structure variables. SIAM J. Appl. Math. 48, 549–591.

Turnbull, L.A., Crawkey, M., Rees, M., 2000. Are plant populations seed-limited? A review of seed sowing experiments. Oikos 88, 225–238.

Valladares, F., 2003. Light heterogeneity and plants: from ecophysiology to species coexistence and biodiversity. In: Esser, K., Lüttge, U., Beyschlag, W., Hellwig, F. (Eds.), Progress in Botany. Springer, Heidelberg, pp. 439–471.

Von Foerster, H., 1959. Some remarks on changing populations. In: Stohlman, F. (Ed.), The Kinetics of Cellular Proliferation. Grune and Stratton, New York, pp. 382–407.

Webb, G.F., 1985. Theory of Nonlinear Age-Dependent Population Dynamics. Marcel Dekker, New York.

Zavala, M.A., Bravo de la Parra, R., 2005. A mechanistic model of tree competition and facilitation for Mediterranean forests: scaling from leaf physiology to stand dynamics. Ecol. Modelling 188, 76–92.